

1 **Electrolysis of low-grade and saline surface water**

2

3 W. Tong¹, M. Forster², F. Dionigi³, S. Dresp³, R. Sadeghi Erami¹, P. Strasser^{3*}, A. J. Cowan^{2*},
4 P. Farràs^{1*}

5 ¹School of Chemistry, National University of Ireland Galway, Galway, Ireland; ²Department of Chemistry and
6 Stephenson Institute for Renewable Energy, University of Liverpool, Liverpool, UK; ³The Electrochemical
7 Energy, Catalysis and Materials Science Laboratory, Department of Chemistry, Chemical Engineering Division,
8 Technical University Berlin, Berlin, Germany

9

10 **Abstract**

11 Powered by renewable energy sources such as solar, marine, geothermal and wind, generation
12 of storable hydrogen fuel through water electrolysis provides a promising path towards energy
13 sustainability. However, state-of-the-art electrolysis requires support from associated processes
14 such as desalination of water sources, further purification of desalinated water, and
15 transportation of water, which often contribute financial and energy costs. One strategy to avoid
16 these operations is to develop electrolyzers that are capable of operating with impure water
17 feeds directly. Here we review recent developments in electrode materials/catalysts for water
18 electrolysis using low-grade and saline water, a significantly more abundant resource
19 worldwide compared to potable water. We address the associated challenges in design of
20 electrolyzers, and discuss future potential approaches that may yield highly active and selective
21 materials for water electrolysis in the presence of common impurities such as metal ions,
22 chloride and bio-organisms.

23

24 **Introduction**

25 Freshwater is likely to become a scarce resource for many communities, with more than 80%
26 of the world's population exposed to high risk levels of water security.¹ This has been
27 recognised within the Sustainable Development Goal 6 (SDG 6) on Clean Water and
28 Sanitation.² At the same time, low-grade and saline water is a largely abundant resource which,
29 used properly, can address SDG 7 on Affordable and Clean Energy as well as SDG 13 on
30 Climate Action.

31

32 Hydrogen, a storable fuel, can be generated through water electrolysis and it may provide
33 headway towards combating climate change and reaching zero emissions,³ since the cycle of

34 generation, consumption and regeneration of hydrogen can achieve carbon neutrality. In
35 addition to providing a suitable energy store, hydrogen can be easily distributed and used in
36 industry, households and transport. Hydrogen and the related fuel cell industry has the potential
37 to bring positive economic and social impacts to local communities in terms of energy
38 efficiency and job markets; globally the hydrogen market is expected to grow 33% to \$155
39 billion in 2022.⁴ However, there are remaining challenges related to the minimisation of the
40 cost and integration of hydrogen into daily life, as well as meeting the ultimate hydrogen cost
41 targets of <2 US\$/kg set by U.S. Department of Energy.⁵⁻⁷

42 Commercially available water electrolyzers operate with support from ancillary
43 components/equipment.^{8,9} The high purity water feeds are achieved by incorporating extensive
44 water purification systems into the overall electrolyser design (internal) or via pre-treatment
45 using external purification/desalination plants. Desalination and subsequent purification, and
46 the associated investment costs for plantation, land, maintenance, and transportation, therefore
47 impose considerable costs. Several techno-economic studies have been published in the last
48 few years,^{10,11} however, a more comprehensive review with up-to-date costs is still needed.
49 Desalination costs vary considerably depending on the price of electricity, and increase if
50 intermittent renewable sources are used.¹² Nevertheless, the cost of water purification systems
51 remains significant.¹² Particular interest in direct saline water electrolysis exists for off-shore
52 large-scale hydrogen production, a sector where the capital costs are dominated by the footprint
53 of the installation, and the simplification in engineering by removing pre-treatment systems
54 would have a great impact on the economic viability of such installations.³

55 A route to reduce cost would be to use low-grade or saline water directly through development
56 of efficient and selective catalytic electrode materials and the utilisation of effective
57 membranes in the electrolyzers that are suitable for impure water. Therefore, ideal catalytic
58 electrode materials and membranes should be able to deal with competing redox reactions at
59 both electrodes, complications related to membrane function, reactor degradation and
60 biofouling. Here we review key issues and recent research in electrolysis and the development
61 of electrode materials/catalysts targeting direct use of low-grade and saline water in the
62 electrolysis processes. In addition, we address the major aspects in the design of electrolyzers
63 for hydrogen generation.

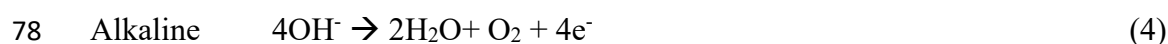
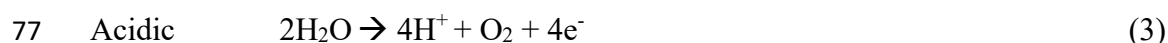
64

65 **Challenges of saline water electrolysis**

66 Splitting water into oxygen and hydrogen is an energetically uphill chemical process where an
67 external energy source is required to drive the reaction. In an electrolyser, electricity is
68 converted to, and stored in the form of, chemical bonds. The hydrogen evolution reaction (HER)
69 at the cathode is a two electron-proton reaction, which can be formulated as equation (1) or (2)
70 under acidic or alkaline conditions respectively.



73 The counter reaction at the anode, the oxygen evolution reaction (OER), is a multi-electron
74 transferring process, involving several intermediates and the removal of four protons per
75 oxygen molecule evolved. It can be described by equation (3) or (4) in acidic or alkaline
76 environment respectively.



79 Catalysts are usually either deposited onto the current collector electrodes (catalyst coated
80 electrode, CCE,) or are coated directly onto the ion exchange membranes (catalyst coated
81 membrane, CCM) to facilitate the water splitting reactions. An important catalytic activity
82 metric is the difference between the applied potential at a given current density and the half-
83 reaction standard potential; the so called overpotential (η). This difference characterises the
84 extra energy taken to push the half reaction significantly forward from the thermodynamic zero
85 net-current equilibrium point.¹³ The complexity of the OER requires a large overpotential, even
86 with state-of-the-art catalysts and especially when compared to the HER.

87 Water electrolysis typically requires ultra-purified water, either directly in membrane
88 electrolysers (Proton Exchange Membrane water electrolysers, PEMWE; Anion Exchange
89 Membrane water electrolysers, AEMWE) or in a mixture with salts for alkaline water
90 electrolysers (AWE). The key challenges in the direct electrolysis of saline water have long
91 been identified and discussed,¹⁴ and remain major issues today. Although carbonates in
92 seawater (saline water) can act as buffers, the capacity is not high enough to prevent increases
93 in the local pH at the cathode and decreases in the local pH at the anode. Studies showed
94 changes in pH near the electrode surface could be on the order of 5-9 pH units from that of the
95 bulk seawater, even at moderate current densities $< 10 \text{ mA cm}^{-2}$.¹⁵⁻¹⁷ Such dramatic pH
96 fluctuations may cause catalyst degradation. Local pH increases near the cathode during
97 seawater (not artificially buffered) electrolysis can lead to precipitation of magnesium

98 hydroxide ($Mg(OH)_2$), which occurs when $pH \geq \sim 9.5$,¹⁸ blocking the cathode.^{14,19} Stabilization
99 of pH fluctuations may require the addition of supporting electrolytes.^{20,21}

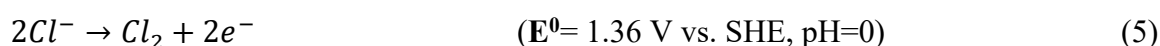
100 Other challenges include the presence of non-innocent ions (both anions and cations)^{17,22} and
101 bacteria/microbes²³, as well as small particulates, all of which may poison electrodes/catalysts
102 and limit their long-term stability. This challenge also extends to the membranes used for the
103 separation of the anode and cathode.²⁴ Another key issue to consider is the competition between
104 the OER and chloride chemistry at the anode.

105 Chloride electro-oxidation chemistry is complicated and several reactions occur depending on
106 the pH values, potentials applied, and temperature. If, for simplicity, we consider the
107 temperature of 25 °C and fix the total concentration of chlorine species to 0.5 M (a typical
108 chloride concentration for seawater), a Pourbaix diagram for aqueous chloride chemistry can
109 be constructed as shown in Figure 1.¹⁷

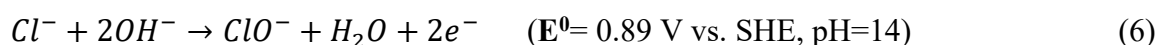
110 When the pH is below 3.0 the free chlorine evolution reaction (CIER, Eq. 5) dominates over
111 the other chloride oxidation reactions (see Figure 1). Hypochlorous acid formation might also
112 occur at lower pH at high anodic potentials, but becomes the major reaction for pH 3-7.5.
113 Hypochlorite formation takes place at pH values higher than 7.5 (Eq. 6), which represents the
114 pK_a of hypochlorous acid. Partial dissociations (i.e. chlorine dissolved in water) and
115 disproportionation (i.e. hypochlorite ions subjected to higher temperature) complicate the
116 chemistry of chlorine species. At the two pH extremes the two chloride oxidation reactions are:

117

118 CIER:



119 Hypochlorate formation:



120 The competing chloride oxidations are thermodynamically unfavourable compared to the OER
121 (Figure 1) and the difference between the standard electrode potentials increases with
122 increasing pH until the hypochlorite formation starts, where it remains at its maximum value
123 of ~ 480 mV.¹⁷ In other words, under alkaline conditions a water oxidation catalyst can exhibit
124 up to 480 mV kinetic overpotential without any interfering chlorine chemistry. This is known
125 as the “alkaline design criterion”¹⁷ in saline water electrolysis, because the requirements for
126 the catalytic activity of the OER catalyst are least stringent in this region.

127 It is worth noting that both chloride reactions (5) and (6) are two-electron reactions, in contrast
128 with the OER in which four electrons are involved. This difference in the numbers of electrons
129 involved in the mechanisms (2 versus 4) give rise to the commonly observed higher
130 overpotential for OER than chloride oxidation and makes OER kinetically unfavourable.
131 Therefore, developing highly selective anode catalysts is essential to avoid the evolution of
132 corrosive and toxic chlorine gas during the electrolysis of saline water.

133 **Reactor design considerations**

134 Currently the two proven low-temperature (<100 °C) water electrolyser technologies
135 dominating the commercial market are AWE and PEMWE.²⁵ Other emerging technologies
136 include low temperature AEMWE,²⁶ as well as high-temperature electrolysis, such as Proton
137 Conducting Ceramic electrolysis (~150 °C – 400 °C)²⁷ and Solid Oxide electrolysis (~500 -
138 800 °C).²⁸ These four configurations are depicted in Figure 2.

139 These electrolyser technologies use either ultra-pure, deionized 18 MΩ water or 20-30% KOH
140 aqueous solution (AWE) with contaminants at and below the ppm level. Such high levels of
141 water purity are chosen to avoid complications related to catalyst operation, membrane
142 operation, and general component degradation. The severity of the challenges associated with
143 use of impure water depends to some degree on the electrolysis configurations.

144 PEMWE contain a solid acid polymer electrolyte²⁹ (e.g. Nafion®) between the anode and
145 cathode. In most cases, the water feed is only supplied to the anode, where it is oxidised to
146 form O₂ and H⁺. Protons then migrate through the PEM towards the HER catalyst (cathode).
147 In this approach, the low pH medium provided by the PEM complicates the anode chemistry
148 and OER selectivity over chloride oxidation reactions becomes challenging. In addition, as a
149 type of cation transporter, the commonly used Nafion® membrane is vulnerable to foreign ions,
150 especially cationic impurities which can be trapped and concentrated, leading to a reduction in
151 proton conductivity.^{25,30} The PEM may isolate certain impurities at the anode, however cationic
152 species such as metal ions and Mg²⁺ will still migrate from the anode to reach the cathode. It
153 is possible to feed water only to the cathode thus minimising any interaction between chloride
154 ions and the anode. In this case water migrates through the membrane where it is oxidised,
155 protons transfer back to the cathode where H₂ is produced.³¹ However, migration of electrolyte
156 and impurities towards the anode will still occur to some degree. Due to transport through the
157 membrane both configurations are likely to result in contact between impurities and the cathode,
158 potentially leading to metal or salt deposition.

159 An AWE operates as a 2-compartment cell separated by a porous diaphragm that allows
160 hydroxyl ion (OH^-) migration while preventing gas crossover. A liquid alkaline electrolyte is
161 pumped around both sides of the cell and water is reduced at the cathode into H_2 and OH^- . OH^-
162 then migrates through the diaphragm towards the anode where O_2 formation occurs. Diaphragm
163 materials for AWE such as Zirfon[®] are reported to be more physically robust and less
164 susceptible to blockages compared to membranes (PEM/AEM).³² In contrast to PEM and AEM
165 that largely block either anions or cations, respectively, both types of species, such as H^+ , Na^+ ,
166 OH^- and Cl^- , are able to migrate through the diaphragm, which should be kept in consideration
167 for system design. This may be problematic if it lowers the transference numbers of the most
168 mobile ions.

169 In an AEMWE, the anion exchange membrane is sandwiched between the anode and cathode.
170 Water can be supplied to the cathode, the anode or both sides. H_2 and OH^- are generated at the
171 cathode and OH^- migrates through the membrane to the anode where O_2 is produced.²⁶ The
172 membrane itself shares the same limitations with that of AWE related to unwanted migration
173 of anions such as Cl^- , meaning competition between OH^- and Cl^- oxidation is a concern
174 regardless of where the electrolyte is fed.²¹ The high operating pH of both AWE and AEMWE
175 can help to minimise Cl^- oxidation, making them particularly interesting for saline water
176 splitting.

177 High-temperature water electrolyzers include proton conducting ceramic electrolysis (~150-
178 400 °C) and solid oxide electrolysis (~800-1000 °C). Water evaporates and transports to the
179 cathode as steam to produce H_2 . A solid oxide or ceramic membrane selectively passes O^{2-}
180 through to the anode to form O_2 .²⁸ This configuration may provide an opportunity to purify the
181 water source (generating ‘clean’ steam) before it reaches the catalyst and membrane.³³
182 Therefore, this technology has the potential to open up the design window beyond electrode
183 materials that are investigated in the other technologies. However, the high operating
184 temperature of means a higher energy demand and a higher operational cost compared to rival
185 technologies that typically operate below 100 °C. In addition, the high temperature limits the
186 type of electrode materials and other electrolyser components to meet the stability requirements
187 for long-term operation. These challenges may prevent their potential installation in offshore
188 facilities coupled to large-scale wind farms, making them more suitable for coastal installation.

189 All four configurations share common problems including physical blockages from solid
190 impurities, precipitates and microbial contaminations affecting either the catalysts or separator

191 material. Thus, a simple filtration of the saline or low-grade water feeds is essential for
192 avoidance of membrane blockages. It may be possible to maintain membrane activity through
193 recovery procedures. For example, periodically resting an electrolyser at open circuit has been
194 shown to recover a portion of lost activity assigned to chloride blocking of the membrane.²¹
195 Metal components are also at risk of corrosion. For example, in a PEM electrolyser the current
196 collectors and separator plates are typically made of titanium, graphite or a coated stainless
197 steel,²⁵ and the lifetime of these materials, particularly in the presence of Cl⁻, should be
198 carefully considered.

199 The chlor-alkali industry can provide some guidance for selecting materials capable of
200 withstanding harsh corrosive environments. Because of its high stability, titanium is chosen
201 for all parts that are in contact with chlorinated water, including the support materials for anode
202 and cathode catalysts. The corrosion resistance of titanium relies on the development of a
203 surface oxide layer. Other useful components used in this industry are Teflon that can be found
204 as a construction component thanks to its inertness, and persulfonated membranes such as
205 Nafion to separate half-cell reactions. However, they are still susceptible to physical
206 damage.^{34,35} To circumvent some of the aforementioned issues, recent studies have shown an
207 interest towards using water vapour (including saline water) as water feeds in both PEMWE
208 and AEMWE.³⁶⁻³⁸ In these cases, air was bubbled through a saline aqueous media to reach high
209 levels of humidity and gas phase electrolysis was conducted. A system composed of buoys that
210 are floating at the ocean surface has been proposed,³⁶ which has the benefit of overcoming the
211 risk of fouling of catalysts and membranes associated with impure liquid water, although the
212 current density is significantly lower than that for liquid-based electrolysers.

213 **Anode materials for electrolysis in impure water**

214 Several strategies have been devised for OER-selective water oxidation anode catalysts that
215 operate in low-grade or saline water. First, the alkaline OER/CIER design criterion has been
216 leveraged, that is, maximising the thermodynamic potential difference between the two
217 catalytic processes by operating the electrolyser in alkaline conditions. This implies the
218 development of highly active OER catalysts designed for alkaline conditions that provide the
219 desired faradaic current at or below 480 mV. The second strategy is the design of OER catalysts
220 for alkaline or acid environments with exclusive selectivity towards the OER due to surface
221 sites of optimised binding of OER intermediates. Third, Cl⁻ blocking layers next to the OER
222 catalyst have been used to prevent the diffusion of Cl⁻ ions from the electrolyte to the surface
223 of the OER catalyst. This Cl⁻ blocking layer may operate in alkaline or acid conditions.

224 **Alkaline design criterion.** The first approach is based on thermodynamic and kinetic
225 considerations, as well as the fact that saline water is essentially a non-buffered electrolyte.
226 Therefore, an additive is likely required to avoid changes in local pH during electrolysis.
227 Kinetic considerations suggest that it is particularly challenging to compete with chloride
228 oxidation due to the more complicated catalytic 4-electron mechanism of the OER, while
229 thermodynamics indicate that alkaline conditions provide a larger potential window where
230 OER is favourable. Based on these reasons, an alkaline catalyst design criterion (Figure 3a)
231 was proposed to achieve 100% OER selectivity in saline water splitting at alkaline pH,
232 provided the overpotentials of the catalysts are lower than ~480 mV at the desired current
233 density (e.g. 500 – 2000 mA cm⁻²).¹⁷

234 It is often difficult to achieve the desired high current densities below an overpotential of 480
235 mV (Mn₂O₃ and Fe₂O₃ in Figure 3b).²⁰ As an additional “criterion”, the overpotential should
236 ideally be as moderate as possible so that it is still less than 480 mV for a given high current
237 density. High performances in Cl⁻-free 0.1 M KOH and 1 M KOH electrolytes have been
238 reported for the family of NiFe oxyhydroxide catalysts,^{17,39,40} which include some of the most
239 active catalysts in alkaline media. An unsupported NiFe LDH catalyst in a membrane electrode
240 assembly (MEA) experimentally confirmed the concept of the criterion, by demonstrating
241 current densities up to 290 mA cm⁻² at under ~480 mV overpotential, which is close to what is
242 required for medium or large size electrolyzers.²¹ The performance loss after 100 hours to about
243 50 – 70 % of the initial activity was attributed to the unsuitability of the membrane rather than
244 to catalyst degradation, which was supported by quasi *in-situ* XAS measurements.

245 As shown in Figure 4a, FeO_x nanomaterials as bifunctional HER/OER catalysts were reported
246 to exhibit OER activity in alkalinised saline water with comparatively lower performances
247 (overpotential of 400 mV at 10 mA cm⁻²).⁴¹ However, such bifunctional HER/OER activities
248 allow realisation of an overall precious metal free electrolyser. Formation of surface redox-
249 active species (iron phosphate) led to significant increases in both catalytic performance and
250 stability in the case of phosphate buffered saline water oxidation by CaFeO_x at pH 7.0 (Figure
251 4b).⁴² Recently, nickel oxide electrodes were also successfully used in alkalinised saline water
252 with 100% OER selectivity.⁴³

253 **Selective OER sites and reaction environments.** The second approach aims to develop
254 catalysts containing active sites that optimise the chemical bonding of the reactive OER
255 intermediates to make them highly OER selective. This approach is feasible in all pH media
256 but also challenging since the sites of OER active catalysts are typically also active for the

257 CIER.⁴⁴ This issue was addressed in several theoretical studies. Calculations on various rutile
258 (110) oxide surfaces confirmed that a linear scaling relationship between the Cl and O
259 adsorption energies exists. This implies that the CIER always requires lower overpotentials
260 than the OER where the scaling holds.⁴⁵ One report showed that on a RuO₂ (110) surface the
261 kinetic volcano plot of the CIER is flatter than that of the OER,⁴⁶ which was related to the
262 number of intermediates. The tips of both volcano plots are very close and for this reason as
263 well as the predictions of linear scaling relationships, it is not feasible to improve the OER
264 selectivity where it dominates over CIER. Fundamentally, new types of sites are necessary to
265 break the scaling relationships and so to enable sites with higher OER selectivity.

266 Experimental investigations of OER selective saline water splitting catalysts have focused on
267 Co and Ru based systems. Co-based OER catalysts are subjects of intense investigations due
268 to their performance at neutral pH with presence of a phosphate buffer. This is particularly
269 appealing for saline water oxidation as the average pH of saline water is close to neutral. Co-
270 Pi, an electrodeposited Co-based catalyst from a phosphate electrolyte, can sustain selective
271 OER in phosphate electrolyte containing 0.5 M NaCl (pH 7.0) at 1.30 V (vs NHE,
272 corresponding to ~483 mV overpotential) at current densities comparable to NaCl-free
273 electrolyte (greater than 0.9 mA cm⁻²). Only 2.4% of the charge passed in a 16 h experiment
274 was attributed to oxidised chloride species.⁴⁷

275 When mixed with Carbon (Vulcan[®] XC-72) and deposited on Ti mesh electrodes, Co-Fe LDH
276 nanoparticles exhibited a Faradaic efficiency of 94 ± 4% in simulated saline water (3.5 %
277 salinity, pH=8.0). Only 0.06% of the total charge passed was attributed to oxidised chloride
278 species after an 8h controlled potential experiment at a constant overpotential of 560 mV.⁴⁸
279 The improved OER performance in saline water was attributed to a synergistic effect of the
280 multiple ions contained in saline water and CoFe LDH (Figure 4c), i.e. complex multiple ions
281 in seawater can mediate proton transfers in concert with electron-transfer reactions.⁴⁸ Co-based
282 selenide electrodes obtained by selenisation of Co foils were also tested in phosphate buffered
283 saline water (pH= 7.09), with superior performance to the reference Ir-C/Pt-C (Figure 4d).⁴⁹
284 These examples highlight the relevance of operating close to the neutral/alkaline design
285 criterion to achieve high OER selectivity. The concept of tuning the relative reaction rates of
286 key steps of the OER and the chloride oxidation reactions is an important strategy toward OER
287 selective sites or site environments. For instance, the use of non-innocent elements such as iron
288 and selenium can facilitate proton transfer on the reactive interfaces. However, the fundamental
289 mechanistic origin of these observations in saline water still await further clarification.

290 Ru based catalysts have shown selectivity for both OER and CIER. While most of the Ru based
291 studies had a focus on the CIER^{35,50-53} or the fundamental understanding of the CIER on
292 ruthenium titanium oxide (RTO),^{46,54-56} there are a few studies that reported enhanced
293 selectivity towards OER on some Ru-based catalysts. Some speculated that doping of Zn into
294 RuO₂ crystal structure caused a rearrangement of the local atomic structure in the vicinity of
295 the Zn ions, enhancing the oxygen evolution process at positive potentials and, overall,
296 improving the selectivity of the OER in chloride containing acidic media.⁵⁷ Additional work is
297 required to confirm and clarify the origins of the enhanced OER selectivity in all the above
298 experimental reports. This involves state-of-art and novel emerging *in situ* and *operando*
299 electrocatalytic studies of the structure and chemical state of the catalytic interface during the
300 catalysis, combined with time-resolved studies of the OER and CIER reaction product onset
301 and formation rates.⁵⁸⁻⁶¹

302 For a different system, DFT calculations have predicted transition metal hexacyanometallates
303 (MHCMs), such as Prussian blue (PB, Fe₄[Fe(CN)₆]₃ nH₂O) and its analogues to be highly
304 energy efficient and selective OER catalyst materials.⁶² In this context, a thin shell of MHCM
305 provides good catalytic activity while the conductive core of basic cobalt carbonate (BCC)
306 facilitates efficient charge transfer. This material in a triple-junction solar cell achieved 17.9 %
307 solar to hydrogen conversion efficiency in saline water at neutral pH. The addition of NaCl (50
308 mM NaCl, 0.1 M phosphate buffer at pH 7.0) into the electrolyte enhanced the water oxidation
309 rate by Ru(II) polypyridyl complexes.⁶³

310 ***Ct blocking layer.*** In order to circumvent the overpotential limitations that are imposed by
311 thermodynamics for a selective OER catalyst surface in the presence of Cl⁻ ions, an approach
312 based on the application of a protecting MnO_x electrode coating was employed (Figure 5a).⁶⁴
313 The study on Mn based catalysts for saline water oxidation started with the report of MnO₂ on
314 a dimensionally stable anode (DSA) obtaining OER selectivity of 99%.¹⁴ γ -MnO₂ type multi-
315 metallic catalysts were investigated systematically for the OER-selective water oxidation in
316 0.5 M NaCl aqueous solution at various pH (1-10), with all of them showing efficiency higher
317 than 90%. These catalysts included Mn-W,⁶⁵ Mn-Mo,⁶⁶⁻⁶⁸ Mn-Mo-W,⁶⁹⁻⁷¹ Mn-Mo-Fe^{70,72} and
318 Mn-Mo-S.^{73,74}

319 The electrode architecture consisted of Mn-based catalysts on iridium oxide coated Ti substrate
320 electrodes. The purpose of the iridium oxide intermediate layer was the protection of the Ti
321 substrate from the formation of insulating TiO₂. Rutile-type Ir_{1-x}Sn_xO₂ was found as the most
322 effective intermediate layer,⁷³ even though the oxidation of the Ti substrate could not be

323 entirely prevented. This led to an increased overpotential for $\text{Mn}_{1-x-y}\text{Mo}_x\text{Sn}_y\text{O}_{2+x}$ after
324 electrolysis for 1000 hours at 100 mA cm^{-2} in 0.5 M NaCl solution at pH 1.^{73,74} A study on Ir_{1-x}
325 Sn_xO_2 without coating of Mn-based catalysts confirmed that Ti oxidation is unavoidable, even
326 though protection could be tuned by varying element composition and calcination
327 temperature.⁷⁵ In these studies, the OER catalytically active phase is considered to be the Mn-
328 based outer layer even though IrO_2 is an active OER catalyst.

329 A recent study showed MnO_x overlayers play the role of blocking the diffusion of Cl^- to the
330 Ir-based intermediate layer, since iridium oxides are also known as excellent CIER catalysts.⁶⁴
331 Using an electrodeposited MnO_x thin film on glassy carbon-supported hydrous iridium oxide
332 (IrO_x/GC) in aqueous chloride solutions of pH ~ 0.9 ,⁶⁴ the enhanced OER selectivity by the
333 presence of the MnO_x layer was confirmed in 30 mM Cl^- solution (Figure 5b). It was concluded
334 that MnO_x was not involved in the OER mechanism, but rather acted as a Cl^- diffusion barrier,
335 while remaining permeable to water (Figure 5a).

336 However, MnO_x is known to act as OER catalyst itself, becoming OER active at somewhat
337 more anodic potentials above $+1.6 \text{ V}_{\text{RHE}}$. Thus, it is feasible that at more anodic overpotentials
338 the protecting MnO_x layer may not only become active for OER, but may also start catalysing
339 the CIER.⁴⁴ This speculation, however, needs experimental validation. In addition, locally very
340 acidic pH conditions at the MnO_x layer may lead to detrimental corrosion. The presented
341 electrode performances of MnO_x coated electrodes are lower compared to the Mn-free IrO_x
342 electrode (Figure 5b), which could be due to the limited water diffusion through the
343 catalytically inert MnO_x layer.⁶⁴ The use of such blocking layers should be optimised to prevent
344 such negative effects from happening.

345 Another approach to suppress CIER involves coating OER catalysts such as NiFeO_x and CoO_x
346 with a permselective cerium oxide layer. This has allowed water oxidation to proceed whilst
347 remaining impermeable to Cl^- , amongst other small ions and molecule contaminations.⁷⁶
348 Similarly, a cation-selective layer (Nafion[®]) on IrO_x electrodes can prevent Cl^- ion from
349 approaching the IrO_x electrode and improve the oxygen production (in a 0.5 M NaCl solution
350 at pH 8.3).⁷⁷ The advantage of this approach is the catalytic inertness of Nafion compared to
351 MnO_x and CeO_x . Note that the operating cell voltages at 100 mA cm^{-2} were reported to be ~ 3.2
352 V greater compared to conventional alkaline water electrolyzers, possibly due to the lower
353 conductivity of NaCl solution compared to KOH solution.

354 Cathodes for H_2 evolution

355 In contrast to water oxidation at the anode, the primary concerns for the operation of a cathode
356 in impure water do not relate to low Faradaic efficiencies, but are instead based upon the long-
357 term stability of HER electrocatalysts in the presence of impurities which can lead to active
358 site blocking and corrosion. Both saline and surface fresh water contain high levels of
359 undesirable cationic species, including Ca^{2+} and Mg^{2+} , which are known to deposit at the
360 cathode as hydroxides under reductive conditions, and current density losses of >50 % have
361 been reported due to salt deposition after short periods of operation (24 hours).^{19,78} The cathode
362 surface can also be affected through reduction and electrodeposition of dissolved ions such as
363 Cu, Cd, Sn and Pb under reaction conditions.⁷⁹ The extent to which competing cathode
364 reactions involving metal cations occur will depend on the applied potential window and the
365 specific ions present. Lab-scale studies typically use purified saline solutions (only NaCl) or
366 electrolytes of known compositions. Further studies which address in detail the role of specific
367 impurities such as salts or metals on electrode activity would be highly beneficial to the
368 community.

369 The changing composition of both sea and surface fresh water worldwide represents a
370 challenge when trying to pinpoint specific impurities and it would be beneficial for the
371 community to agree on a standardised seawater composition for testing. Solid impurities and
372 microbial contaminations which are typically not present in synthetic electrolytes also require
373 attention and may lead to further reductions in activity by physically blocking the catalyst
374 surface. Key approaches to improve stability at the cathode include the potential use of
375 membranes to prevent impurities reaching the cathode through an engineering approach (e.g.
376 PEM electrolyzers); the development of catalysts with surface sites selective to HER and
377 resistant to side reactions/deactivation; and the deposition of permselective overlayers on top
378 of the catalyst to block impurities whilst allowing the transfer of reagents and products.

379 ***pH design criterion.*** Pt is currently regarded as the benchmark HER electrocatalyst, in both
380 acid and alkali conditions. Plots of catalytic rate versus metal-hydrogen (M-H) binding energy
381 (Volcano plots⁸⁰) show that Pt achieves a near optimal level of activity leading to it being the
382 common choice for PEMWE where an acidic environment is provided by the membrane.^{9,25}
383 However the cost of Pt is high and alkaline electrolyzers typically use Ni or Ni-based metal
384 alloys (such as NiMo, NiMoCo and NiFe) for the HER due to their lower cost and stability at
385 low pH environments.^{9,25,63} There is a significant interest in the development of new H_2
386 evolution electrocatalysts to act as cost effective alternatives to expensive catalysts such as
387 Pt.⁸¹ We refer the reader to recent studies highlighting the range of high-performance

388 electrocatalysts for HER identified in recent years covering a wide operating pH range.^{39,63} In
389 almost all cases these examples have yet to be tested in low-grade or saline water.

390 From the perspective of cathode performance, PEMWE provides an optimal pH for HER due
391 to the high local concentration of H⁺ supplied by the membrane.²⁹ A PEMWE configuration
392 could also protect the cathode from impurities by acting as a filtration barrier as depicted in
393 Figure 6b, provided a highly selective membrane can be found. However, a PEMWE
394 configuration provides a minimal overpotential window and does not satisfy the OER operation
395 conditions for avoiding Cl₂ production at the anode. Given that a successful saline water
396 splitting device will likely have to operate in near neutral to alkaline (pH>8) conditions the
397 following discussions focus on neutral to alkali HER catalysis. Finding HER catalysts which
398 can operate efficiently in neutral to alkaline conditions also provides an opportunity to target
399 cheaper earth abundant elements such as Ni, Mn and Fe which are typically unstable in acidic
400 conditions.⁸²

401 ***HER catalyst selectivity and stability.*** Table 1 provides a summary of HER electrodes that
402 have been tested for low-grade, saline or seawater. The studies presented in Table 1 have
403 assessed their systems using different criteria and as such direct comparison is difficult. This
404 highlights the need for standard criteria when assessing potential catalysts in seawater
405 applications.

406 It is notable that many of the cathodes reported in Table 1 have focused on using saline water
407 at/near neutral pH; exceptions include Pt, Ni-Fe-C and FeO_x cathodes that have been tested in
408 alkaline media in the presence of Cl⁻. Pt has been operated as a cathode in an alkaline
409 electrolyser containing 0.5 M NaCl.²¹ A loss of current density of ~50% was reported after 100
410 hours of continuous operation. This loss was proposed to be due to deterioration of the alkali
411 membrane conductivity rather than catalysts deactivation. A 4 hour rest period every 20 hours
412 was found to lead to a recovery effect. The system was not tested in real seawater, however the
413 results in NaCl did not indicate cathode failure. A carbon content and grain size study of Ni-
414 Fe-C electrodes⁸³ was carried out in electrolyte containing 3.5% NaCl solution at 90 °C and pH
415 = 12. The electrocatalysts with the maximum carbon content (1.59%) and minimum grain size
416 (3.4 nm) was shown to possess the lowest overpotential for HER.

417 Bifunctional catalysts capable of operating as both anode and cathode are attractive as this
418 simplifies cell construction, and could also allow for electrochemical regeneration by potential
419 switching as in the case of FeO_x bi-functional material in KOH (pH = 13).⁴¹ Reversing the

420 anode and cathode every 1 hour by potential switching prevents (entirely within error) catalyst
421 activation loss.⁴¹ Similar results were achieved for iron foil electrodes, in which addition of 0.6
422 M NaCl to the system revealed quantitative water splitting with 2:1 generation of H₂:O₂,
423 however testing was not carried out in real seawater.

424 Earth abundant HER catalysts⁸² have recently been reported for electrolysis in neutral media.
425 Catalysts consisting of a Cu surface modified by Ni atoms and CrO_x clusters were prepared
426 through anisotropic doping of the metal surface and have been proposed to asymmetrically
427 destabilise bonds in the water molecule to favour its dissociation into H⁺ and OH⁻. NiMoS has
428 been evaluated and proposed as a potential cathode material for operation in saline water at
429 neutral pH.^{62,84} When combined with a MHCM-z-BCC anode the system operated for 100
430 hours in neutral buffered saline water with minimal current density decline.

431 Corrosion due to Cl⁻ and related Cl⁻ oxidation products such as Cl₂ can be a concern for
432 electrode stability. While chloride oxidation products are primarily a concern for the anode,
433 gas crossover is possible,⁸⁵ and the stability of the cathode in the presence of chloride and
434 oxidation products such as Cl₂ should be carefully considered. Crossover can be managed to
435 an extent by controlling membrane thickness to find a suitable balance between separation
436 properties and conductivity, and by controlling pressure gradients. Alloys of either Pt or Ni
437 with transition metals including Cr, Fe, Co and Mo (i.e. PtM and NiM) have been shown to
438 reduce corrosion leading to metal chloride formation in saline water and in the presence of Cl₂,
439 increasing long-term stability.⁸⁶⁻⁸⁹ PtMo⁸⁹ and PtRuMo⁸⁶ alloys on Ti mesh have shown
440 excellent performance in real seawater with <10% loss of their original current density after
441 172 hours of operation. NiMo^{87,88} alloys have also been shown to provide a promising
442 combination of catalytic activity and long-term stability. The increased corrosion resistance of
443 these alloys is attributed to competitive dissolution reactions between the guest M species with
444 Cl₂.⁸⁶ Alloys containing Mo are also widely reported in more traditional water splitting
445 applications to possess favourable overpotentials and stability.^{63,90} Development of catalysts
446 capable of inherently resisting corrosion or poisoning due to foreign ion deposition such as
447 described above are desirable in order to achieve long-term stability as exemplified in Figure
448 6c.

449 **Blocking layers.** Addition of permselective barrier layers on catalyst surfaces have been
450 demonstrated to limit unwanted Cl⁻ chemistry at the anode,⁹¹ and a similar approach could be
451 envisaged for protecting cathode materials to enhance long-term stability, as shown in Figure

452 6d. Several examples of cathode protecting layers have been demonstrated recently. A thin
453 layer of $\text{Cr}(\text{OH})_3$ coated onto a Pt cathode has been reported to act as a selective blocking layer,
454 providing selectivity for the HER over competing hypochlorate reduction in the chlorate
455 process.^{92,93} MnO_x has also been suggested to play a similar role to that of $\text{Cr}(\text{OH})_3$.^{64,94} A
456 graphitic shell around a CoMoP electrocatalyst has been shown to promote HER performance
457 and provide protection against etching, agglomeration and poisoning in saline water.⁹⁵
458 Furthermore, it is possible that permselective layers could play a dual role in electrolyser
459 systems, by protecting both the catalysts layer and also any membrane which sits underneath
460 the catalyst. Although mass transport issues may arise upon the addition of a permselective
461 overlayer, such an approach could provide a significant improvement to the long-term stability
462 of a system operating in impure water.

463 **Conclusions and outlook**

464 Several issues need attention for electrolysis of impure or saline water to become viable. The
465 use of appropriate membranes is crucial for building an efficient electrolyser using seawater or
466 low-grade water without extensive purification/treatments. Common membrane and
467 diaphragm technologies are susceptible to transport of and blockage by foreign ions, however
468 the effect this has on the activity and longevity of a system is not fully understood and further
469 research into membrane blockage by impurities would be highly valuable.

470 At the anode, overcoming the competition between chlorine chemistry and water oxidation is
471 essential for successful saline water splitting. Oxygen evolution selectivity can be obtained by
472 operating in alkaline conditions, and this has been demonstrated in highly alkaline systems (pH
473 ~ 13) containing NaCl. However, a transition to real seawater at high pH is expected to have
474 additional challenges associated with precipitation formation when seawater is adjusted to pH
475 greater than ~ 10 .¹⁸ Based on the Pourbaix diagram, there may be an opportunity to operate near
476 pH 8-9 and maintain O_2 selectivity. In this scenario careful control of pH becomes a vital task
477 and a strong buffer is likely required. Other strategies for operating anodes and cathodes in
478 impure water include selective transport of ions by membranes, formation of permselective
479 materials/barriers onto the surface of catalysts, and finding electrode materials with
480 catalytically selective sites to favour desired reactions over side-reactions and catalysts
481 poisoning.

482 It would be beneficial for the community to assess new materials for use in impure water using
483 standardised criteria. The composition of real seawater is complex and varies around the globe,

484 and the use of a standardised electrolyte composition (e.g. Instant Ocean) for benchmarking
 485 new catalyst materials is important. For buffered saline water, a similar standard should be
 486 employed along with a clearly defined nature and concentration of the buffer species. Other
 487 relevant parameters which also need standardisation include long-term stability assessment
 488 (>100 hours) at a standard current density (10 mA cm⁻² in batch systems, 200 mA cm⁻² in flow
 489 electrolysis cells).

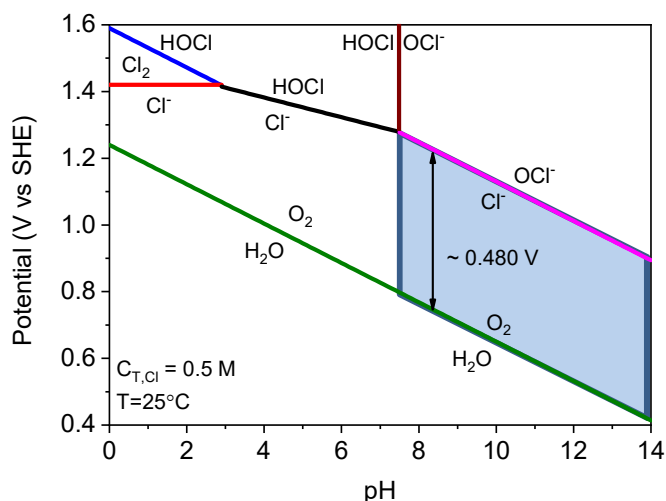
490 Some electrocatalysts are already available with good activity and selectivity,^{24,92} but long-
 491 term stability remains an issue. For membranes, an interesting approach could be to mimic
 492 electrokinetic membranes found in certain plants such as mangrove roots that filter seawater,
 493 thereby reducing saline concentration on the surface of the electrode, and minimise membrane
 494 fouling or decomposition.⁹⁶

495 The transformation towards a decarbonised society requires careful considerations in reducing
 496 the cost. In most cases, saline water electrolyser technologies will need to have competitive
 497 capital and operational costs (CAPEX and OPEX) compared to electrolyser technologies
 498 coupled to desalination and purification units. Extra revenue may be obtainable if a careful
 499 management of the waste stream is utilised.⁹⁷ We believe that islands can be ideal places to test
 500 new technologies given the abundance of renewable energy and the desire for storage and self-
 501 sufficiency,⁹⁸ combined with the inherent current costs of importing fossil fuels not available
 502 in these territories. Although it remains unclear which of the electrolyser technologies will be
 503 more suitable for saline waters, the operation at near neutral pH (7-9) is preferable and AEM
 504 would most likely fulfil this requirement, unless gas-phase electrolysis becomes competitive.

Table 1: H₂ evolution electrocatalysts reported in saline electrolyte

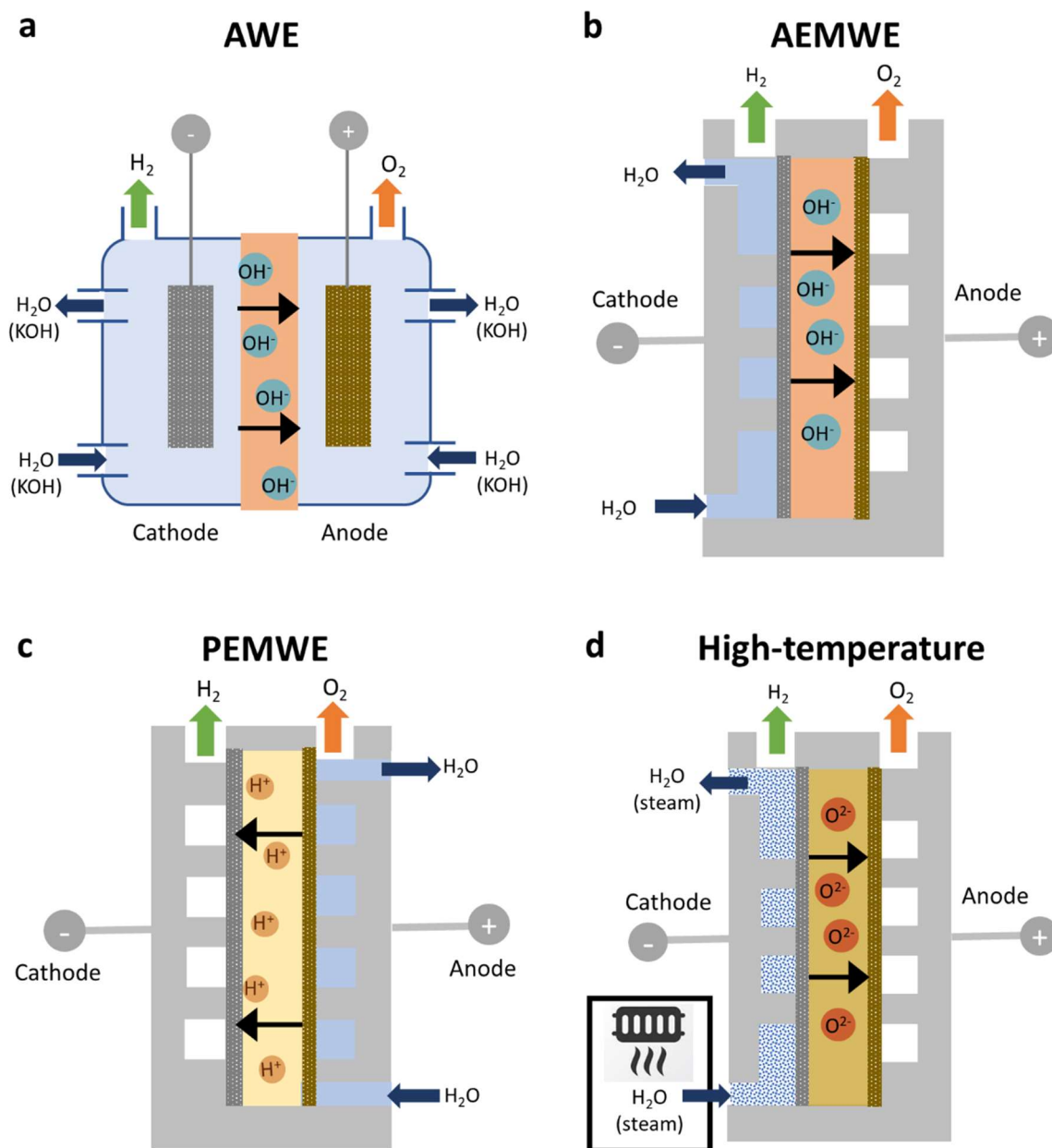
Catalyst	Support	Electrolyte	Cell setup	Ref
Pt	Pt plate	Neutral buffered seawater.	phosphate natural 1-compartment, 2-electrode cell with IrO ₂ on carbon cloth counter electrode.	62
Pt nanoparticles: Pt 46.7 wt% with carbon black	Spray coated onto Tokuyama A201 membrane	0.1 M KOH + 0.5 M NaCl.	Membrane electrode assembly with Ni-Fe layered double hydroxide anode material spray coated onto reverse.	21
NiMoS	Carbon fibre cloth	Neutral buffered seawater.	phosphate natural 1-compartment, 2-electrode cell with MHCM-z-BCC counter electrode.	62
Nanostructured NiMoS	Carbon fibre cloth	Natural seawater, pH = 8.07.	1-compartment, 3-electrode cell with graphite foil counter electrode.	84

Ni-M (M^{1/4} Co, Cu, Mo, Au, Pt)	Ti mesh			Natural seawater, filtered to remove large particulates.	3-electrode system with Pt sheet counter electrode and Ag/AgCl reference electrode.	88
Pt-M (M^{1/4} Cr, Fe, Co, Ni, Mo)	Ti mesh			Natural seawater.	3-electrode system with a platinum sheet counter electrode and Ag/AgCl reference electrode.	89
FeO_x	FTO glass slide			0.6 M NaCl + 0.1 M KOH, pH = 13.	2-electrode, 2-compartment setup, FeO _x counter-reference electrode, Nafion [®] 117 membrane.	41
Mn doped NiO/Ni	Ni-foam			Natural seawater, pH = 8.2.	1-compartment, 3-electrode cell with graphite rod counter electrode and SCE reference electrode.	78
Urea-derived carbon nanotubes	Drop-cast glassy carbon electrode	onto carbon		Natural seawater with phosphate buffer, pH=7.	1-compartment, 3-electrode cell with carbon rod counter electrode and SCE reference electrode.	99
CoMoP with 2-4 layer graphitic carbon shell	Drop cast glassy carbon electrode	onto carbon		Natural seawater, filtered, pH = 8.35.	1-compartment, 3-electrode configuration with graphite rod counter electrode and SCE reference electrode.	100
Ni-Fe-C	Etched substrate	steel		3.5% NaCl solution at 90 °C, pH = 12.	1-compartment, 3 electrode cell with Pt plate counter electrode and Hg/HgO (1 M NaOH) reference electrode.	83
CoSe and Co₃Se₈	Cobalt foil			Phosphate buffered natural seawater.	1 compartment, 3-electrode cell with carbon counter electrode and Ag/AgCl reference electrode.	49
Co₃Mo₃C/carbon nano tubes	Ni foam			Natural seawater, filtered.	3-electrode cell, 1-compartment, with platinum sheet counter electrode and Ag/AgCl reference electrode.	101
Mo₅N₆	Drop-cast glassy carbon	onto		Natural seawater, pH~8.4.	3-electrode cell, 1-compartment, Graphite rod counter electrode and Ag/AgCl reference electrode, constant flow of Ar to remove gas build up.	102
Co-S	FTO glass slide			Natural seawater with 1 M NaClO ₄ .	3-electrode, medium frit separated 2-compartment cell, with FTO counter electrode and Ag/AgCl reference electrode.	103
NiNS	Ni foam			Natural seawater with phosphate buffer, pH = 7.05.	2-electrode cell with NiNS as anode and cathode.	104



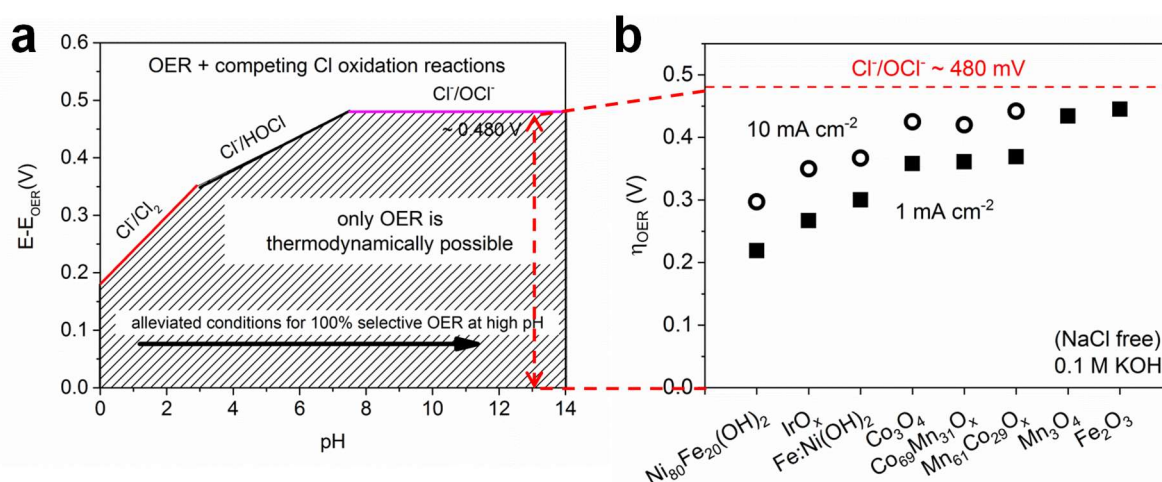
506

507 **Figure 1: The Pourbaix diagram of an aqueous saline electrolyte.** Represented as the
 508 electrode potential vs pH diagram, it provides information of the stability of an aqueous 0.5 M
 509 NaCl electrolyte, including the H₂O/O₂ and the Cl⁻/Cl₂/HOCl/ClO⁻ redox couples. The diagram
 510 depicts potential-pH regions where the oxygen evolution reaction (OER) and the chloride
 511 oxidation reactions are thermodynamically possible. The green line represents the
 512 thermodynamic equilibrium between water and oxygen. At electrode potentials more positive
 513 of the green line, the OER process becomes thermodynamically possible. The red line shows
 514 the competing acidic oxidation of chloride to free gaseous chlorine. The black and purple lines
 515 mark the onset of the oxidation of chloride to hypochlorous acid, HOCl, or hypochlorite, ClO⁻.
 516 The potential difference between the chloride chemistry and the water oxidation is maximised
 517 to 480 mV in alkaline media pH > 7.5 (light blue region), where chloride is oxidised to ClO⁻.
 518 Adapted with permission from ref. ¹⁷, John Wiley and Sons.



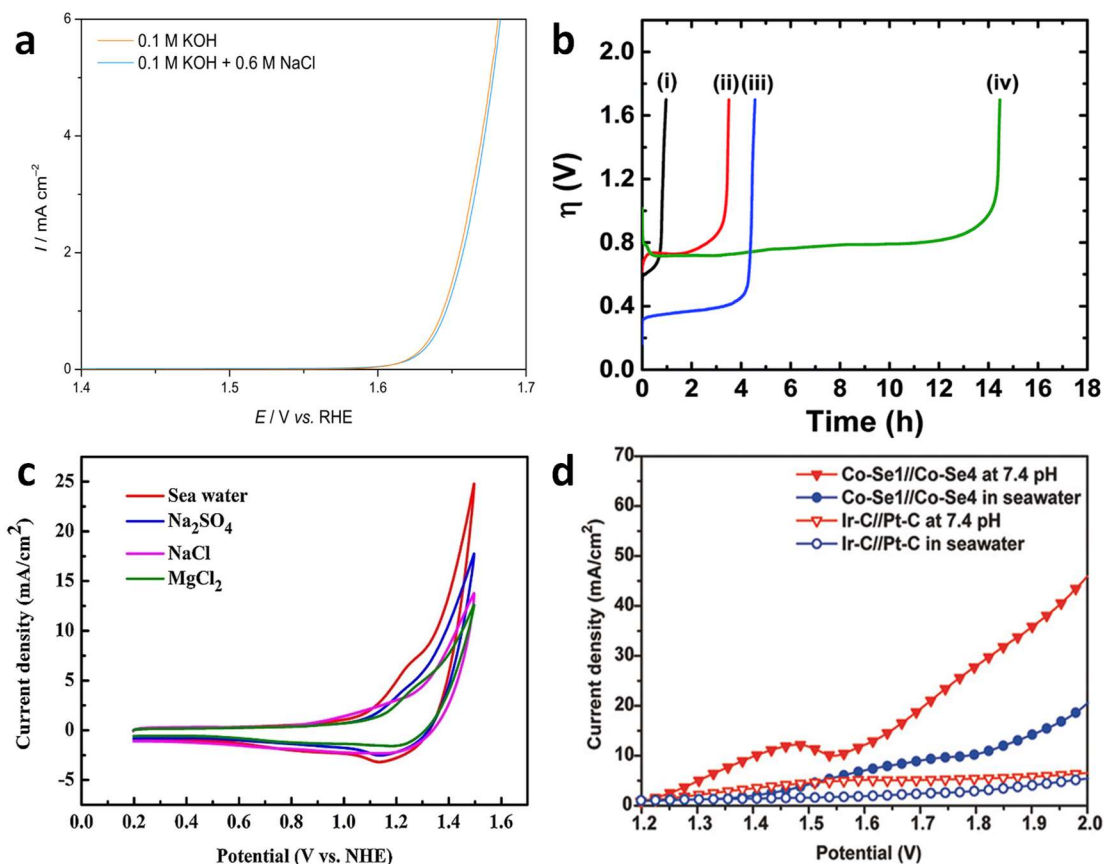
519

520 **Figure 2. Leading configurations for water electrolysis.** **a**, An alkaline water electrolyser
 521 (AWE) operates as a 2-compartment cell in which a liquid alkaline electrolyte (typically 20-
 522 30% KOH) is pumped around both sides and a porous diaphragm allows hydroxyl ion (OH⁻)
 523 migration while preventing gas crossover. **b**, An anion exchange membrane water electrolyser
 524 (AEMWE) sandwiches an OH⁻ transporting membrane between the anode and cathode. Water
 525 is supplied to the cathode in this example, however it is also possible to supply water to the
 526 anode or both sides. **c**, A proton exchange membrane water electrolyser (PEMWE) consists of
 527 a solid acid electrolyte polymer sandwiched between the anode and cathode. In most cases,
 528 water is only fed to the anode. **d**, High-temperature water electrolysis includes proton
 529 conducting ceramic electrolysis (~150-400 °C) and solid oxide electrolysis (~800-1000 °C).
 530 Water evaporates and transports to the cathode as steam to produce H₂ while a solid oxide or
 531 ceramic membrane transports O²⁻ to the anode.

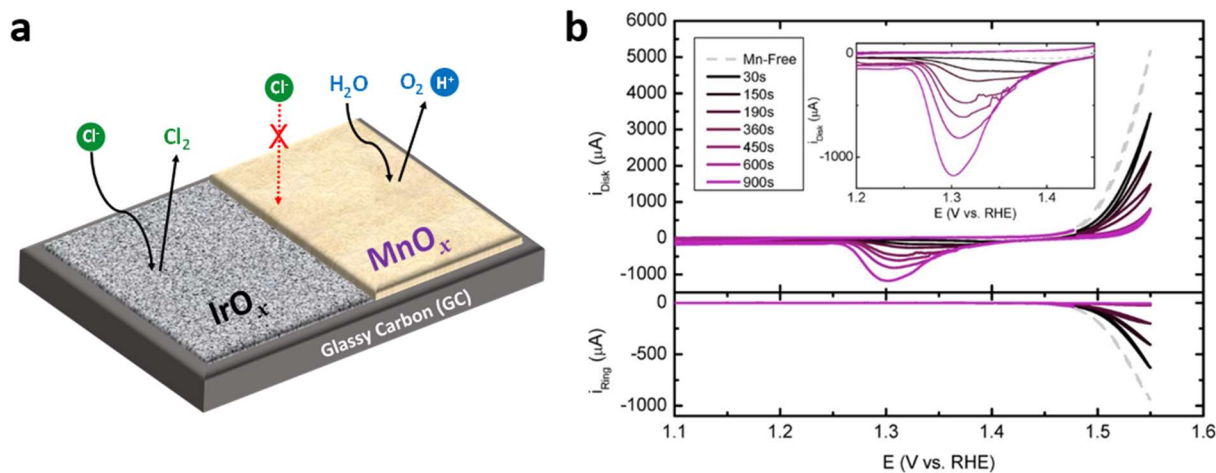


532
533

534 **Figure 3. Experimental implementation of the alkaline design criterion of saline water**
 535 **splitting.** **a**, Predicted maximally allowed kinetic overpotentials (derived from thermodynamic
 536 Pourbaix diagrams) of OER electrocatalyst as function of pH to realise 100% selective water
 537 splitting. **b**, Experimental OER overpotentials of supported oxide catalysts in O₂ saturated 0.1
 538 M KOH compared with reference IrO_x/C catalyst evaluated at the current density of 1 mA cm⁻²
 539 ² (full symbols) and 10 mA cm⁻² (open symbols). The red dashed lines show the overpotential
 540 limit in alkaline conditions (alkaline design criterion) of ~480 mV. While many catalysts fulfil
 541 the design criterion at low current densities (1 mA cm⁻²), this becomes challenging for
 542 moderately higher current densities such as 10 mA cm⁻². Mn₃O₄ and Fe₂O₃, for instance, do no
 543 longer fulfil the design criterion at 10 mA cm⁻² and hence would start generating detrimental
 544 ClO⁻ by-products. Figure 3a is adapted with permission from ref. ¹⁷, John Wiley and Sons;
 545 Figure 3b summarises data reported in ref. ^{17,20}.



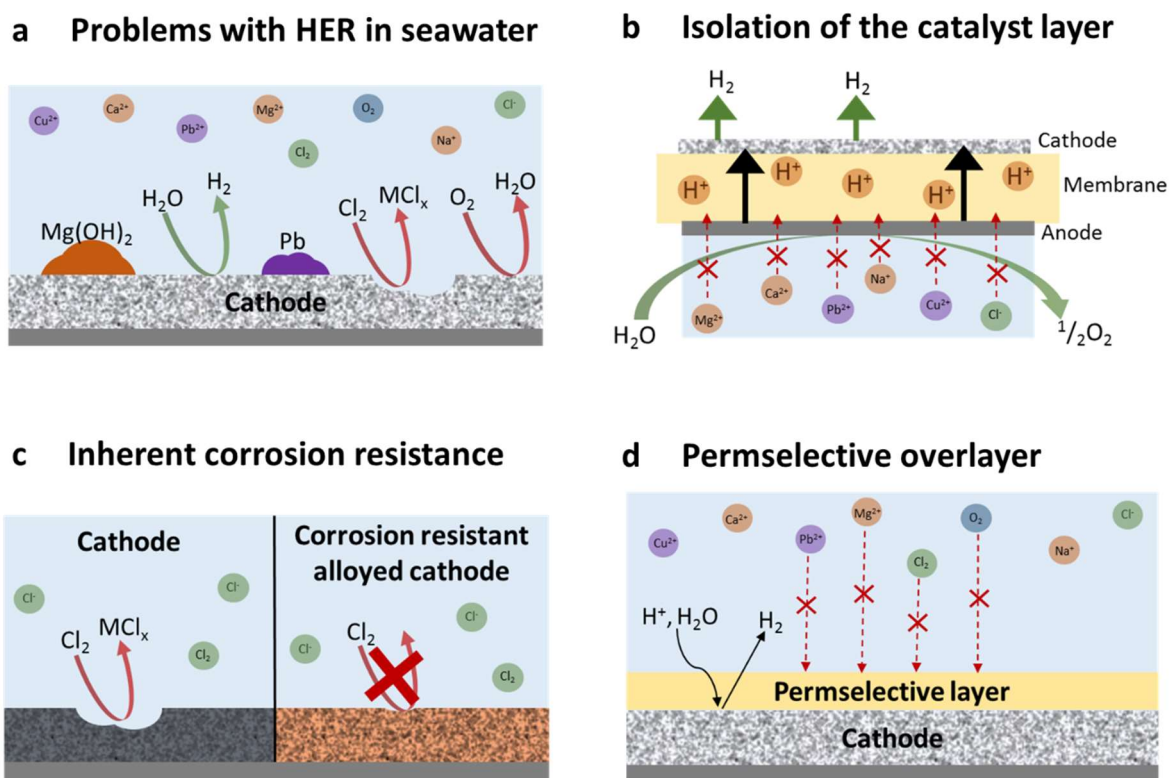
546
 547 **Figure 4. Water oxidation activity and stability of oxide catalysts and influence of anionic**
 548 **and cationic contaminations.** **a**, OER selectivity in alkaline artificial seawater electrolyte
 549 solution. Linear Sweep Voltammetry (LSV) of a FeO_x electrode operated in 0.1 M KOH and
 550 (0.6 M NaCl + 0.1 M KOH) electrolytes. **b**, Overpotential transients of different materials at
 551 10 mA cm^{-2} in phosphate buffered (0.5 M, pH 7) saline water under N_2 atmosphere. **c**, CVs of
 552 Co-Fe LDH/GCEs in saline water and aqueous solutions including MgCl_2 , NaCl or Na_2SO_4 as
 553 electrolytes. Scan rate: 100 mV s^{-1} . **d**, Polarisation curves of Co-Se₁//Co-Se₄ and Ir-C//Pt-C
 554 in buffered saline water at a scan rate of 5 mV s^{-1} . The counter and reference electrodes were
 555 Pt mesh and Ag/AgCl respectively. *iR* compensation is used. Figure (a) reproduced from the
 556 supporting information of ref. ⁴¹, John Wiley and Sons, Open access. Other figures
 557 reproduced/reprinted with permission from (b) ref.⁴², Royal Chemical Society; (c) ref. ⁴⁸,
 558 Elsevier; (d) ref. ⁴⁹, John Wiley and Sons.



559

560
 561
 562
 563
 564
 565
 566
 567
 568
 569

Figure 5. Selective OER catalysts by Cl⁻ blocking overlayers. **a**, Illustration of MnO_x deposited onto IrO_x decreases the ClER selectivity in the presence of 30 mM Cl⁻ from 86% to less than 7%, making it a highly OER-selective catalyst. **b**, Top panel exhibits CVs of an IrO_x/GC rotating disk electrode in 0.5 M KHSO₄, 30 mM KCl (pH = 0.88), and 0.6 mM MnSO₄ (0 for the Mn²⁺-free experiment). Rotation rate: 1500 rpm. MnO_x films were preconditioned at 1.48 V before initiating the forward scan at 1.48 V. The inset shows the details of CVs for potentials between 1.2 and 1.5 V. The lower panel shows the corresponding *i*_{Ring} (*E*_{Ring} = 0.95 V). Figures adapted/reproduced with permission from ref. ⁶⁴, American Chemical Society.



570

Figure 6. Challenges and potential solutions to improve long-term stability of HER in low-grade water. **a**, Challenges for cathode operation in low-grade or saline water are in particular related to reduced stability due to deposition of impurities such as metal ions and hydroxides, and corrosion of the catalyst. **b**, Separation of the catalyst from the water source by a suitable membrane or through reactor design could prevent catalyst deactivation. **c**, Development of catalysts with inherent corrosion resistance or selective surface chemistry are desirable if long-term stability is to be maintained. **d**, Use of a permselective overlayer on top of the catalyst or on top of the membrane can prevent unwanted species from reaching the catalyst surface while also allowing normal catalytic function to occur.

580

581 **References**

582 1. Vörösmarty, C. J. *et al.* Global threats to human water security and river biodiversity.
 583 *Nature* **467**, 555–561 (2010).
 584 2. Spröte, W. *ECOSOC – Economic And Social Council. A Concise Encyclopedia of the*

- 585 *United Nations 07404*, (2010).
- 586 3. IEA. *The future of hydrogen*. (2019).
- 587 4. Bezdek, R. H. The hydrogen economy and jobs of the future. *Renew. Energy Environ.*
588 *Sustain.* **4**, 1 (2019).
- 589 5. Moliner, R., Lázaro, M. J. & Suelves, I. Analysis of the strategies for bridging the gap
590 towards the Hydrogen Economy. *Int. J. Hydrogen Energy* **41**, 19500–19508 (2016).
- 591 6. Deutsch, T. G. & Turner, J. A. *2014 U.S. DOE Hydrogen & Fuel Cells Program*
592 *Review*. (2014).
- 593 7. Ramsden, T., Ruth, M., Diakov, V., Laffen, M. & Timbario, T. A. *Hydrogen*
594 *Pathways: Updated Cost, Well-to-Wheels Energy Use, and Emissions for the Current*
595 *Technology Status of Ten Hydrogen Production, Delivery, and Distribution Scenarios*.
596 (2013). doi:10.2172/1107463
- 597 8. Ursúa, A., Gandía, L. M. & Sanchis, P. Hydrogen production from water electrolysis:
598 Current status and future trends. *Proc. IEEE* **100**, 410–426 (2012).
- 599 9. Xiang, C., Papadantonakis, K. M. & Lewis, N. S. Principles and implementations of
600 electrolysis systems for water splitting. *Mater. Horizons* **3**, 169–173 (2016).
- 601 10. Matute, G., Yusta, J. M. & Correas, L. C. Techno-economic modelling of water
602 electrolyzers in the range of several MW to provide grid services while generating
603 hydrogen for different applications: A case study in Spain applied to mobility with
604 FCEVs. *Int. J. Hydrogen Energy* **44**, 17431–17442 (2019).
- 605 11. Chardonnet, C. *et al.* *Study on Early Business Cases for H₂ in Energy Storage and*
606 *More Broadly Power To H₂ Applications*. EU Commission (2017).
- 607 12. Karagiannis, I. C. & Soldatos, P. G. Water desalination cost literature: review and
608 assessment. *Desalination* **223**, 448–456 (2008).
- 609 13. Fourmond, V., Jacques, P. A., Fontecave, M. & Artero, V. H₂evolution and molecular
610 electrocatalysts: Determination of Overpotentials and effect of homoconjugation.
611 *Inorg. Chem.* **49**, 10338–10347 (2010).
- 612 14. Bennett, J. E. Electrodes for generation of hydrogen and oxygen from seawater. *Int. J.*
613 *Hydrogen Energy* **5**, 401–408 (1980).

- 614 15. Katsounaros, I. *et al.* The effective surface pH during reactions at the solid-liquid
615 interface. *Electrochem. commun.* **13**, 634–637 (2011).
- 616 16. Auinger, M. *et al.* Near-surface ion distribution and buffer effects during
617 electrochemical reactions. *Phys. Chem. Chem. Phys.* **13**, 16384–16394 (2011).
- 618 17. Dionigi, F., Reier, T., Pawolek, Z., Gliech, M. & Strasser, P. Design Criteria,
619 Operating Conditions, and Nickel-Iron Hydroxide Catalyst Materials for Selective
620 Seawater Electrolysis. *ChemSusChem* **9**, 962–972 (2016).
- 621 18. Kapp, E. M. The Precipitation of Calcium and Magnesium from Sea Water by Sodium
622 Hydroxide. *Biol. Bull.* **55**, 453–458 (1928).
- 623 19. Kirk, D. W. & Ledas, A. E. Precipitate formation during sea water electrolysis. *Int. J.*
624 *Hydrogen Energy* **7**, 925–932 (1982).
- 625 20. Dresp, S. & Strasser, P. Non-Noble Metal Oxides and their Application as Bifunctional
626 Catalyst in Reversible Fuel Cells and Rechargeable Air Batteries. *ChemCatChem* **10**,
627 4162–4171 (2018).
- 628 21. Dresp, S. *et al.* Direct Electrolytic Splitting of Seawater: Activity, Selectivity,
629 Degradation, and Recovery Studied from the Molecular Catalyst Structure to the
630 Electrolyzer Cell Level. *Adv. Energy Mater.* **8**, 1800338 (2018).
- 631 22. Adbel-Aal, H. K. & Hussein, I. A. Parametric study for saline water electrolysis: Part
632 1-hydrogen production. *Int. J. Hydrogen Energy* **18**, 485–489 (1993).
- 633 23. Oh, B. S. *et al.* Formation of hazardous inorganic by-products during electrolysis of
634 seawater as a disinfection process for desalination. *Sci. Total Environ.* **408**, 5958–5965
635 (2010).
- 636 24. Dresp, S., Dionigi, F., Klingenhof, M. & Strasser, P. Direct Electrolytic Splitting of
637 Seawater: Opportunities and Challenges. *ACS Energy Lett.* **4**, 933–942 (2019).
- 638 25. Carmo, M., Fritz, D. L., Mergel, J. & Stolten, D. A comprehensive review on PEM
639 water electrolysis. *Int. J. Hydrogen Energy* **38**, 4901–4934 (2013).
- 640 26. Vincent, I. & Bessarabov, D. Low cost hydrogen production by anion exchange
641 membrane electrolysis: A review. *Renew. Sustain. Energy Rev.* **81**, 1690–1704 (2018).
- 642 27. Meng, Y. *et al.* Review: recent progress in low-temperature proton-conducting

- 643 ceramics. *J. Mater. Sci.* **54**, 9291–9312 (2019).
- 644 28. Laguna-Bercero, M. A. Recent advances in high temperature electrolysis using solid
645 oxide fuel cells: A review. *J. Power Sources* **203**, 4–16 (2012).
- 646 29. Mauritz, K. A. & Moore, R. B. State of Understanding of Nafion. *Chem. Rev.* **104**,
647 4535–4586 (2004).
- 648 30. Chae, K. J. *et al.* Mass transport through a proton exchange membrane (Nafion) in
649 microbial fuel cells. *Energy and Fuels* **22**, 169–176 (2008).
- 650 31. Müller, M. *et al.* Water management in membrane electrolysis and options for
651 advanced plants. *Int. J. Hydrogen Energy* **44**, 10147–10155 (2019).
- 652 32. Schalenbach, M., Lueke, W. & Stolten, D. Hydrogen diffusivity and electrolyte
653 permeability of the Zirfon PERL separator for alkaline water electrolysis. *J.*
654 *Electrochem. Soc.* **163**, 1480–1488 (2016).
- 655 33. Lim, C. K., Liu, Q., Zhou, J., Sun, Q. & Chan, S. H. High-temperature electrolysis of
656 synthetic seawater using solid oxide electrolyzer cells. *J. Power Sources* **342**, 79–87
657 (2017).
- 658 34. Hine, F., O’Brien, T. F. & Bommaraju, T. V. *Handbook of Chlor-Alkali Technology,*
659 *Volume I: Fundamentals.* Springer Science & Business Media (2005).
- 660 35. Karlsson, R. K. B. & Cornell, A. Selectivity between Oxygen and Chlorine Evolution
661 in the Chlor-Alkali and Chlorate Processes. *Chem. Rev.* **116**, 2982–3028 (2016).
- 662 36. Kumari, S., Turner White, R., Kumar, B. & Spurgeon, J. M. Solar hydrogen
663 production from seawater vapor electrolysis. *Energy Environ. Sci.* **9**, 1725–1733
664 (2016).
- 665 37. Heremans, G. *et al.* Vapor-fed solar hydrogen production exceeding 15% efficiency
666 using earth abundant catalysts and anion exchange membrane. *Sustain. Energy Fuels*
667 **1**, 2061–2065 (2017).
- 668 38. Kida, T. *et al.* Water Vapor Electrolysis with Proton-Conducting Graphene Oxide
669 Nanosheets. *ACS Sustain. Chem. Eng.* **6**, 11753–11758 (2018).
- 670 39. McCrory, C. C. L. *et al.* Benchmarking Hydrogen Evolving Reaction and Oxygen
671 Evolving Reaction Electrocatalysts for Solar Water Splitting Devices. *J. Am. Chem.*

- 672 *Soc.* **137**, 4347–4357 (2015).
- 673 40. Gong, M. *et al.* An Advanced Ni–Fe Layered Double Hydroxide Electrocatalyst for
674 Water Oxidation. *J. Am. Chem. Soc.* **135**, 8452–8455 (2013).
- 675 41. Martindale, B. C. M. & Reisner, E. Bi-Functional Iron-Only Electrodes for Efficient
676 Water Splitting with Enhanced Stability through in Situ Electrochemical Regeneration.
677 *Adv. Energy Mater.* **6**, 1502095 (2016).
- 678 42. Huang, W.-H. & Lin, C.-Y. Iron phosphate modified calcium iron oxide as an efficient
679 and robust catalyst in electrocatalyzing oxygen evolution from seawater. *Faraday*
680 *Discuss.* **215**, 205–215 (2019).
- 681 43. Juodkazytė, J. *et al.* Electrolytic splitting of saline water: Durable nickel oxide anode
682 for selective oxygen evolution. *Int. J. Hydrogen Energy* **44**, 5929–5939 (2019).
- 683 44. Trasatti, S. Electrocatalysis in the anodic evolution of oxygen and chlorine.
684 *Electrochim. Acta* **29**, 1503–1512 (1984).
- 685 45. Hansen, H. A. *et al.* Electrochemical chlorine evolution at rutile oxide (110) surfaces.
686 *Phys. Chem. Chem. Phys.* **12**, 283–290 (2010).
- 687 46. Exner, K. S., Anton, J., Jacob, T. & Over, H. Controlling selectivity in the chlorine
688 evolution reaction over RuO₂-based catalysts. *Angew. Chemie - Int. Ed.* **53**, 11032–
689 11035 (2014).
- 690 47. Surendranath, Y. & Dinca, M. Electrolyte-Dependent Electrosynthesis and Activity of
691 Cobalt-Based Water Oxidation Catalysts. *J. Am. Chem. Soc.* **131**, 2615–2620 (2009).
- 692 48. Cheng, F. *et al.* Synergistic action of Co-Fe layered double hydroxide electrocatalyst
693 and multiple ions of sea salt for efficient seawater oxidation at near-neutral pH.
694 *Electrochim. Acta* **251**, 336–343 (2017).
- 695 49. Zhao, Y. *et al.* Charge State Manipulation of Cobalt Selenide Catalyst for Overall
696 Seawater Electrolysis. *Adv. Energy Mater.* **8**, 1801926 (2018).
- 697 50. Zeradjanin, A. R., Menzel, N., Schuhmann, W. & Strasser, P. On the faradaic
698 selectivity and the role of surface inhomogeneity during the chlorine evolution reaction
699 on ternary Ti-Ru-Ir mixed metal oxide electrocatalysts. *Phys. Chem. Chem. Phys.* **16**,
700 13741–13747 (2014).

- 701 51. Macounová, K., Makarova, M., Jirkovský, J., Franc, J. & Krtíl, P. Parallel oxygen and
702 chlorine evolution on Ru_{1-x}Ni_xO_{2-y} nanostructured electrodes. *Electrochim. Acta* **53**,
703 6126–6134 (2008).
- 704 52. Kishor, K., Saha, S., Parashtekar, A. & Pala, R. G. S. Increasing Chlorine Selectivity
705 through Weakening of Oxygen Adsorbates at Surface in Cu Doped RuO₂ during
706 Seawater Electrolysis. *J. Electrochem. Soc.* **165**, J3276–J3280 (2018).
- 707 53. Arikawa, T., Murakami, Y. & Takasu, Y. Simultaneous determination of chlorine and
708 oxygen evolving at RuO₂/Ti and RuO₂-TiO₂/Ti anodes by differential
709 electrochemical mass spectroscopy. *J. Appl. Electrochem.* **28**, 511–516 (1998).
- 710 54. Karlsson, R. K. B., Hansen, H. A., Bligaard, T., Cornell, A. & Pettersson, L. G. M. Ti
711 atoms in Ru_{0.3}Ti_{0.7}O₂ mixed oxides form active and selective sites for
712 electrochemical chlorine evolution. *Electrochim. Acta* **146**, 733–740 (2014).
- 713 55. Exner, K. S., Anton, J., Jacob, T. & Over, H. Chlorine Evolution Reaction on
714 RuO₂(110): Ab initio Atomistic Thermodynamics Study - Pourbaix Diagrams.
715 *Electrochim. Acta* **120**, 460–466 (2014).
- 716 56. Sohrabnejad-Eskan, I. *et al.* Temperature-Dependent Kinetic Studies of the Chlorine
717 Evolution Reaction over RuO₂(110) Model Electrodes. *ACS Catal.* **7**, 2403–2411
718 (2017).
- 719 57. Petrykin, V., Macounova, K., Shlyakhtin, O. A. & Krtíl, P. Tailoring the selectivity for
720 electrocatalytic oxygen evolution on ruthenium oxides by zinc substitution. *Angew.*
721 *Chemie - Int. Ed.* **49**, 4813–4815 (2010).
- 722 58. Nong, H. N. *et al.* A unique oxygen ligand environment facilitates water oxidation in
723 hole-doped IrNiO_x core-shell electrocatalysts. *Nat. Catal.* **1**, 841–851 (2018).
- 724 59. Bergmann, A. *et al.* Unified structural motifs of the catalytically active state of
725 Co(oxyhydr)oxides during the electrochemical oxygen evolution reaction. *Nat. Catal.*
726 **1**, 711–719 (2018).
- 727 60. Beermann, V. *et al.* Real-time imaging of activation and degradation of carbon
728 supported octahedral Pt–Ni alloy fuel cell catalysts at the nanoscale using in situ
729 electrochemical liquid cell STEM. *Energy Environ. Sci.* **12**, 2476–2485 (2019).
- 730 61. Fabbri, E., Abbott, D. F., Nachttegaal, M. & Schmidt, T. J. Operando X-ray absorption

- 731 spectroscopy: A powerful tool toward water splitting catalyst development. *Curr.*
732 *Opin. Electrochem.* **5**, 20–26 (2017).
- 733 62. Hsu, S.-H. *et al.* An Earth-Abundant Catalyst-Based Seawater Photoelectrolysis
734 System with 17.9% Solar-to-Hydrogen Efficiency. *Adv. Mater.* **30**, 1707261 (2018).
- 735 63. Zeng, M. & Li, Y. Recent advances in heterogeneous electrocatalysts for the hydrogen
736 evolution reaction. *J. Mater. Chem. A* **3**, 14942–14962 (2015).
- 737 64. Vos, J. G., Wezendonk, T. A., Jeremiase, A. W. & Koper, M. T. M. MnOx/IrOx as
738 Selective Oxygen Evolution Electrocatalyst in Acidic Chloride Solution. *J. Am. Chem.*
739 *Soc.* **140**, 10270–10281 (2018).
- 740 65. Izumiya, K. *et al.* Anodically deposited manganese oxide and manganese-tungsten
741 oxide electrodes for oxygen evolution from seawater. *Electrochim. Acta* **43**, 3303–
742 3312 (1998).
- 743 66. Fujimura, K. *et al.* Anodically deposited manganese-molybdenum oxide anodes with
744 high selectivity for evolving oxygen in electrolysis of seawater. *J. Appl. Electrochem.*
745 **29**, 765–771 (1999).
- 746 67. Fujimura, K. *et al.* Oxygen evolution on manganese-molybdenum oxide anodes in
747 seawater electrolysis. *Mater. Sci. Eng. A* **267**, 254–259 (1999).
- 748 68. Fujimura, K. *et al.* The durability of manganese–molybdenum oxide anodes for
749 oxygen evolution in seawater electrolysis. *Electrochim. Acta* **45**, 2297–2303 (2000).
- 750 69. El-Moneim, A. A., Kumagai, N., Asami, K. & Hashimoto, K. New
751 nanocrystalline manganese-molybdenum-tin oxide anodes for oxygen evolution in
752 seawater electrolysis. *ECS Trans.* **1**, 491–497 (2006).
- 753 70. Matsui, T. *et al.* Anodically deposited Mn-Mo-W oxide anodes for oxygen evolution
754 in seawater electrolysis. *J. Appl. Electrochem.* **32**, 993–1000 (2002).
- 755 71. El-Moneim, A. A. Mn-Mo-W-oxide anodes for oxygen evolution during seawater
756 electrolysis for hydrogen production: Effect of repeated anodic deposition. *Int. J.*
757 *Hydrogen Energy* **36**, 13398–13406 (2011).
- 758 72. Abdel Ghany, N. A., Kumagai, N., Meguro, S., Asami, K. & Hashimoto, K. Oxygen
759 evolution anodes composed of anodically deposited Mn-Mo-Fe oxides for seawater

- 760 electrolysis. *Electrochim. Acta* **48**, 21–28 (2002).
- 761 73. Kato, Z., Bhattarai, J., Kumagai, N., Izumiya, K. & Hashimoto, K. Durability
762 enhancement and degradation of oxygen evolution anodes in seawater electrolysis for
763 hydrogen production. *Appl. Surf. Sci.* **257**, 8230–8236 (2011).
- 764 74. Kato, Z. *et al.* Electrochemical characterization of degradation of oxygen evolution
765 anode for seawater electrolysis. *Electrochim. Acta* **116**, 152–157 (2014).
- 766 75. Kato, Z. *et al.* The influence of coating solution and calcination condition on the
767 durability of Ir_{1-x}Sn_xO₂/Ti anodes for oxygen evolution. *Appl. Surf. Sci.* **388**,
768 640–644 (2016).
- 769 76. Obata, K. & Takanabe, K. A Permselective CeO_x Coating To Improve the Stability of
770 Oxygen Evolution Electrocatalysts. *Angew. Chemie - Int. Ed.* **57**, 1616–1620 (2018).
- 771 77. Balaji, R. *et al.* An alternative approach to selective sea water oxidation for hydrogen
772 production. *Electrochem. commun.* **11**, 1700–1702 (2009).
- 773 78. Lu, X. *et al.* A sea-change: Manganese doped nickel/nickel oxide electrocatalysts for
774 hydrogen generation from seawater. *Energy Environ. Sci.* **11**, 1898–1910 (2018).
- 775 79. Bard, A. J., Parsons, R. & Jordan, J. *Standard Potentials in Aqueous Solution*.
776 (Routledge, 1985). doi:10.1201/9780203738764
- 777 80. Nørskov, J. K. *et al.* Trends in the Exchange Current for Hydrogen Evolution. *J.*
778 *Electrochem. Soc.* **152**, J23 (2005).
- 779 81. Zheng, Y., Jiao, Y., Jaroniec, M. & Qiao, S. Z. Advancing the Electrochemistry of the
780 Hydrogen-Evolution Reaction through Combining Experiment and Theory. *Angew.*
781 *Chemie Int. Ed.* **54**, 52–65 (2015).
- 782 82. Dinh, C.-T. *et al.* Multi-site electrocatalysts for hydrogen evolution in neutral media by
783 destabilization of water molecules. *Nat. Energy* **4**, 107–114 (2019).
- 784 83. Song, L. J. & Meng, H. M. Effect of carbon content on Ni-Fe-C electrodes for
785 hydrogen evolution reaction in seawater. *Int. J. Hydrogen Energy* **35**, 10060–10066
786 (2010).
- 787 84. Miao, J. *et al.* Hierarchical Ni-Mo-S nanosheets on carbon fiber cloth: A flexible
788 electrode for efficient hydrogen generation in neutral electrolyte. *Sci. Adv.* **1**, e1500259

- 789 (2015).
- 790 85. Schalenbach, M. *et al.* Gas Permeation through Nafion. Part 1: Measurements. *J. Phys.*
791 *Chem. C* **119**, 25145–25155 (2015).
- 792 86. Li, H., Tang, Q., He, B. & Yang, P. Robust electrocatalysts from an alloyed Pt-Ru-M
793 (M = Cr, Fe, Co, Ni, Mo)-decorated Ti mesh for hydrogen evolution by seawater
794 splitting. *J. Mater. Chem. A* **4**, 6513–6520 (2016).
- 795 87. Golgovici, F. *et al.* Ni–Mo alloy nanostructures as cathodic materials for hydrogen
796 evolution reaction during seawater electrolysis. *Chem. Pap.* **72**, 1889–1903 (2018).
- 797 88. Zhang, Y., Li, P., Yang, X., Fa, W. & Ge, S. High-efficiency and stable alloyed nickel
798 based electrodes for hydrogen evolution by seawater splitting. *J. Alloys Compd.* **732**,
799 248–256 (2018).
- 800 89. Zheng, J., Zhao, Y., Xi, H. & Li, C. Seawater splitting for hydrogen evolution by
801 robust electrocatalysts from secondary M (M = Cr, Fe, Co, Ni, Mo) incorporated Pt.
802 *RSC Adv.* **8**, 9423–9429 (2018).
- 803 90. Raj, I. A. & Vasu, K. I. Transition metal-based hydrogen electrodes in alkaline
804 solution --- electrocatalysis on nickel based binary alloy coatings. *J. Appl.*
805 *Electrochem.* **20**, 32–38 (1990).
- 806 91. Esposito, D. V. Membrane-Coated Electrocatalysts - An Alternative Approach to
807 Achieving Stable and Tunable Electrocatalysis. *ACS Catal.* **8**, 457–465 (2018).
- 808 92. Vos, J. G. & Koper, M. T. M. Measurement of competition between oxygen evolution
809 and chlorine evolution using rotating ring-disk electrode voltammetry. *J. Electroanal.*
810 *Chem.* **819**, 260–268 (2018).
- 811 93. Lindbergh, G. & Simonsson, D. The Effect of Chromate Addition on Cathodic
812 Reduction of Hypochlorite in Hydroxide and Chlorate Solutions. *J. Electrochem. Soc.*
813 **137**, 3094–3099 (2006).
- 814 94. Endródi, B. *et al.* Towards sustainable chlorate production: The effect of permanganate
815 addition on current efficiency. *J. Clean. Prod.* **182**, 529–537 (2018).
- 816 95. Esswein, A. J., Surendranath, Y., Reece, S. Y. & Nocera, D. G. Highly active cobalt
817 phosphate and borate based oxygen evolving catalysts operating in neutral and natural

- 818 waters. *Energy Environ. Sci.* **4**, 499–504 (2011).
- 819 96. Kim, K., Kim, H., Lim, J. H. & Lee, S. J. Development of a Desalination Membrane
820 Bioinspired by Mangrove Roots for Spontaneous Filtration of Sodium Ions. *ACS Nano*
821 **10**, 11428–11433 (2016).
- 822 97. Kumar, A., Phillips, K. R., Thiel, G. P., Schröder, U. & Lienhard, J. H. Direct
823 electrosynthesis of sodium hydroxide and hydrochloric acid from brine streams. *Nat.*
824 *Catal.* **2**, 106–113 (2019).
- 825 98. Schiermeier, Q., Tollefson, J., Scully, T., Witze, A. & Morton, O. Energy alternatives:
826 Electricity without carbon. *Nature* **454**, 816–823 (2008).
- 827 99. Gao, S. *et al.* Electrocatalytic H₂ production from seawater over Co, N-codoped
828 nanocarbons. *Nanoscale* **7**, 2306–2316 (2015).
- 829 100. Ma, Y. Y. *et al.* Highly efficient hydrogen evolution from seawater by a low-cost and
830 stable CoMoP@C electrocatalyst superior to Pt/C. *Energy Environ. Sci.* **10**, 788–798
831 (2017).
- 832 101. Zhao, Y., Tang, Q., He, B. & Yang, P. Carbide decorated carbon nanotube
833 electrocatalyst for high-efficiency hydrogen evolution from seawater. *RSC Adv.* **6**,
834 93267–93274 (2016).
- 835 102. Jin, H. *et al.* Single-Crystal Nitrogen-Rich Two-Dimensional Mo₅N₆ Nanosheets for
836 Efficient and Stable Seawater Splitting. *ACS Nano* **12**, 12761–12769 (2018).
- 837 103. Sun, Y. *et al.* Electrodeposited cobalt-sulfide catalyst for electrochemical and
838 photoelectrochemical hydrogen generation from water. *J. Am. Chem. Soc.* **135**, 17699–
839 17702 (2013).
- 840 104. Zhao, Y., Jin, B., Vasileff, A., Jiao, Y. & Qiao, S. Interfacial Nickel Nitride/Sulfide as
841 a Bifunctional Electrode for Highly Efficient Overall Water/Seawater Electrolysis. *J.*
842 *Mater. Chem. A* **7**, 8117–8121 (2019).

843

844 **Acknowledgements**

845 W.T., M.F., R.S.D., A.J.C. and P.F. acknowledge financial support from INTERREG Atlantic
846 Area programme (Grant Reference EAPA_190_2016). P.F. acknowledge support from Royal

847 Society Alumni Programme. F.D., S.D. and P.S. gratefully acknowledge financial support by
848 the German Research Foundation (DFG) through Grant Reference Number STR 596/8-1 and
849 the federal ministry for economic affairs and energy (Bundesministerium für Wirtschaft und
850 Energie, BMWi). P.S acknowledges partial financial support by the Cluster of Excellence in
851 Catalysis, UNISYSCAT, funded by the DFG and managed by the Technical University Berlin.

852

853 **Additional information**

854 Reprints and permissions information is available online at www.nature.com/reprints.
855 Correspondence should be addressed to P.F. (pau.farras@nuigalway.ie), A.J.C.
856 (acowan@liverpool.ac.uk) or P.S. (pstrasser@tu-berlin.de).

857

858 **Competing interests**

859 The authors declare no competing interests.